Non-visual opsin expression in the optic tectum of starry flounder (*Platichthys stellatus*)

by

Laurel Aveyard

A Thesis Submitted in Partial Fulfillment of the
Requirements for the Degree of

BACHELOR OF SCIENCE (HONS.)

in the Department of Biology

University of Victoria

Non-visual opsin expression in the optic tectum of starry flounder (*Platichthys stellatus*)

by

Laurel Aveyard

Supervisory Committee

Dr. John Taylor, Supervisor
Department of Biology

Dr. Barbara Hawkins, Honours advisor
Department of Biology

Dr. Robert Chow, External examiner
Department of Biology

Abstract

Non-visual opsins are light sensing proteins that are not associated with the typical image forming process and can be found not only in the retina, but across a wide variety of tissues such as brain and skin. Their expression in the brain specifically has been documented in several species, but the question remains as to whether these proteins are contributing to light sensitivity of the brain itself. The starry flounder (*Platichthys stellatus*) is a species of flatfish with several ecological and anatomical characteristics that allow for an indirect method of investigating the potential of brain light sensitivity. Because of their asymmetrical anatomy, their brains are located with one hemisphere pointing upwards and receiving more light stimulus than the other. They are found as both left sided and right sided individuals in the wild, meaning investigation of light sensitivity related to the upwards facing hemisphere in a given individual is possible. This study investigated expression of the specific non-visual opsin melanopsin in the optic tectum of the brain, which is the structure responsible for integration of visual stimuli. This was done using an immunohistochemical staining technique with antibodies designed to bind mammalian-like melanopsins. This provided a qualitative analysis of the levels of expression and how they differed between the hemispheres. There was no notable qualitative difference found between hemispheres in terms of expression, however there appeared to be pan-neuronal labelling throughout both hemispheres of the optic tectum. Further research is required to identify levels of protein expression, however this is an indication of melanopsin presence in the starry flounder brain and is a first step in understanding how these proteins may function in this asymmetric species.

Table of Contents

Supervisory Committee ii
Abstract iii
Table of Contents iv
List of Tables vi
List of Figures vi
Acknowledgements vii
Introduction 1
Starry flounder anatomy 1
Non-visual opsins 3
Starry flounder ecology 5
Immunohistochemistry 6
Study design and hypothesis 6
Materials and Methods 8
Dissections 8
Antibody tests 8
Sampling 9
Sectioning 11
Optic nerve label 11
Immunolabelling 12
Imaging 13
Results 14
Dissections 14
Antibody tests 14
Starry flounder immunolabelling 17
Additional labelling 24
Discussion 27
Retina 28
Optic tectum labelling 28
Blood vessel labelling 30

Melanopsin in brains ……….………………..…………...……………………..…….….31
Limitations ………..……………………..……………………………………….….32
Future research..……...……………………...……………………………………….….33
Conclusion …………………………………...………………………….………... 34
References …………………………………….……………...………………….……….... 35
Appendix A: Antibody labelling protocol ……………………………………………….....39
Appendix B: Sample measurements and imaging settings …………..……………….……...40

List of tables

Table 1. Overview of samples used …………………….………………………………… 13

Table 2. Overview of antibodies used in this experiment. …………………………………… 13

Table B1. Body measurements of starry flounder samples ……..…………………………… 40

Table B2. Imaging settings……….……………………..……………………………..… 40

List of Figures

Figure 1. Diagram of optic tectum and superior colliculus……………………………………… 2

Figure 2. Phylogenetic tree of mammalian-like melanopsins in teleost fish..……………………4

Figure 3. Labelled brain image and diagram of *Platichthys stellatus* …………………………...14

Figure 4. Immunofluorescent labeling of retina of *Danio rerio* …………....……..……………15

Figure 5. Immunofluorescent labeling of retina of right sided *Platichthys stellatus*…………....16

Figure 6. Immunofluorescent labeling of optic tectum of *Anoplopoma fimbria*……………….. 17

Figure 7. Immunofluorescent labeling of the whole brain of right sided *Platichthys stellatus*….18

Figure 8. Immunofluorescent labeling of optic tectum of right sided *Platichthys stellatus*…..…19

Figure 9. Immunofluorescent labeling of optic tectum of right sided *Platichthys stellatus*…..…20

Figure 10. Immunofluorescent labeling of optic tectum of left sided *Platichthys stellatus*…..…21

Figure 11. Immunofluorescent labeling of optic tectum of left sided *Platichthys stellatus*……..22

Figure 12. Immunofluorescent labeling of optic tectum of right sided *Platichthys stellatus*……23

Figure 13. Immunofluorescent labeling of optic tectum of left sided *Platichthys stellatus* with pas350 primary antibody………………………………………………………………………24

Figure 14. Immunofluorescent labeling of optic tectum sections of *Platichthys stellatus* showing blood vessel labelling.…………………………………………………………………………25

Figure 15. Whole brain of *Platichthys stellatus* with a dye applied to the optic nerve.….…….26

Acknowledgements

I would like to thank my supervisor Dr. John Taylor for accepting me as an Honours student and providing mentorship throughout my research project. This research has taught me many new skills that I wouldn't have otherwise had the chance to learn. Your enthusiasm and guidance helped make the lab environment an inviting place where I could learn without judgement. I am very grateful for the opportunity and will remember my time in the lab fondly.

A big thank you to Isabel Ma for teaching me how to do the immunohistochemical techniques and always being available for my many questions and to share tips. Your continued support and guidance helped me get through the tougher techniques and I appreciate how you were always willing to take time out of your busy schedule to go over something with me.

Thanks to Dr. Bob Chow for training me on the confocal microscope and for access to his cryostat and confocal microscope.

Thank you to Dr. Kerry Delaney for performing the optic nerve labelling procedure.

This research was funded by an NSERC Discovery Grant to Dr. John Taylor. We thank Mike Kattilakoski and the Department of Fisheries and Oceans for permission to collect wild starry flounder.

Lastly, thank you to my parents and sister for all the love and support this past year. I couldn't have done it without you.

Introduction

Starry Flounder Anatomy

The starry flounder (*Platichthys stellatus*) is a species of flatfish in the family *Pleuronectidae*. During metamorphic development, flatfish gradually transition from upright bilaterally symmetrical larvae to adults with a flat body and asymmetrical eye and nare positions (Geffen *et al.,* 2007). Flatfish metamorphosis is a complex and well documented process, having been observed for over 100 years (Kyle, 1923). During development prominent sensory structures migrate, most notably the eye and nare, from what will become the blind side in the mature fish to the eyed side. However, the brain remains in a similar orientation to how it is in the larvae, with one hemisphere facing more upwards and the other one more towards the sea floor (Graf and Baker, 1990). A previous study has investigated differences in protein expression in skin and eye tissues during this period of metamorphosis, and the authors concluded that there are several proteins, particularly those involved in developmental signalling pathways, that have differential expression between the left and right sides of the tissue during development. Most of these proteins are then found to revert to even expression after metamorphic development is complete (Lü *et al.*, 2021). One prominent exception to this is genes involved in skin pigmentation, as these retain their asymmetry with the eyed side having a dark colouration and the blind side becoming white, although several environmental and genetic factors have been suggested to impact this (Kang *et al.* 2014). There are many studies characterizing behaviour and morphology in the starry flounder, however whole genome sequence data for this species is a recent development (Zheng *et al.,* 2025) and studies regarding their cellular and genomic structure are relatively new and ongoing (Lü *et al.*, 2021; Sohn *et al.,* 2025). Due to the recent increase in aquaculture of this species in Asia, current molecular research is primarily focusing on physiology and genetics for populations in artificial environments as that is of most importance to fisheries.

In this study we have investigated the expression of a nonvisual opsin in the starry flounder brain, specifically the optic tectum. The optic tectum in the vertebrate brain, called the superior colliculus in humans, is an important structure for sensory processing of both visual and other sensory stimuli. In humans the structure is small and located in the midbrain, but for fish such as the starry flounder it makes up the largest segment of their brain (Figure 1.).

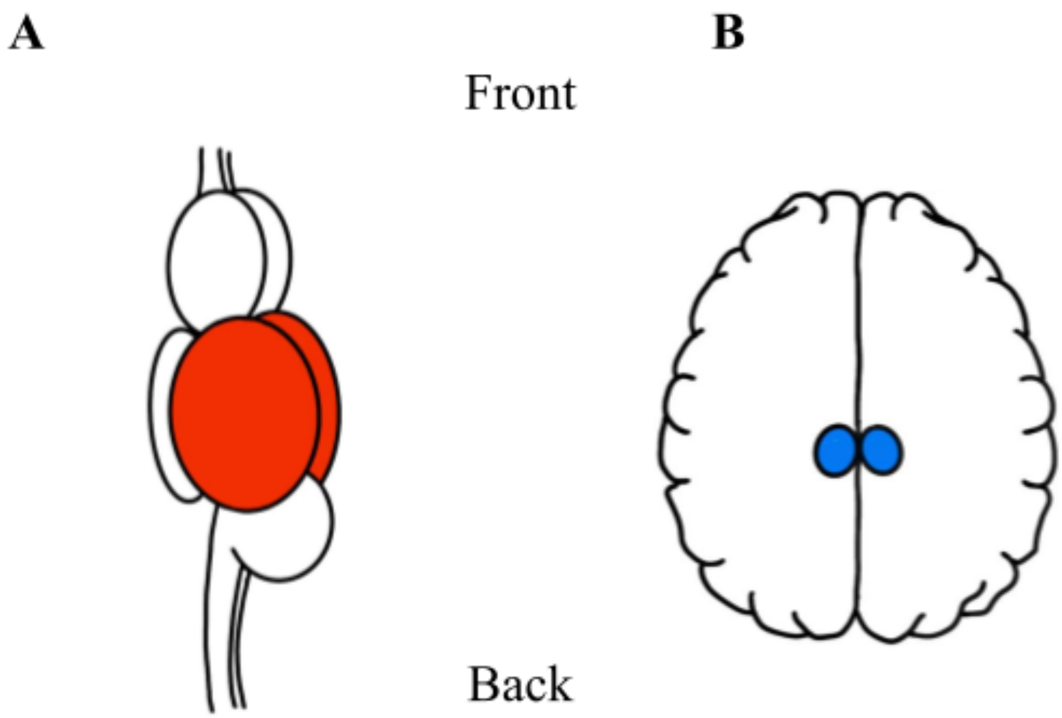

Figure 1. Diagram of optic tectum and superior colliculus region. (A) Top down view of starry flounder brain. Both hemispheres of optic tectum are highlighted in red. (B) Top down view of human brain. Both hemispheres of the superior colliculus are highlighted in blue. Diagram drawn using procreate (version 5.3, Savage Interactive).

Although brain orientation in relation to the body does not shift during flatfish metamorphosis the optic tectum appears to go through a period of asymmetrical growth. Briñon *et al.* (1993) found that in turbot (*Scophthalmus maximus*), different hemispheres of the brain had different volumes during metamorphosis. In the case of the telencephalon, the volume of the hemisphere receiving input from the migratory nare remained reduced once the flatfish reached adulthood. In that study the optic tectum had marked asymmetry with the hemisphere receiving input from the migratory eye being a lower volume during the developmental processes. The two hemispheres of the optic tectum regained their symmetrical volumes once metamorphosis was completed. Briñon *et al.* (1993) speculated that this change in volume was due to the reduced input received from the migratory eye during its movement across the skull. The presence of asymmetries in a wide variety of tissues during development indicate the potential for asymmetries in protein expression in the brain of flatfish.

Non-visual opsins

Non-visual opsins are proteins that are light-sensitive, yet occur in tissues such as skin, brain, liver, and testis, that are not considered to be part of the image formation process. This is a diverse group of proteins, particularly in fish, with over 75% of the 42 opsin genes in the zebrafish genome being classed as non-visual (Davies *et al.,* 2015). There is a great diversity of fishes that are distantly related but possess very similar repertoires of opsin genes. This demonstrates that non-visual opsins stabilised early in the evolution of teleost fish. There are 18 monophyletic subfamilies of non-visual opsin that have been characterised in tetrapods and ray-finned fish (Beaudry *et al.,* 2017). One of these includes the genes belonging to the melanopsin family (*opn4*) (Figure 2.). Melanopsin was first discovered in *Xenopus* skin as a mediator of light dependent melanophore pigment granule dispersal (Provencio *et al.,* 1998). Since its discovery, melanopsin has been investigated in various organisms including zebrafish and mice (Bellingham *et al.,* 2002; Sikka *et al.,* 2014). One of its key functions is mediated through its presence in intrinsically photosensitive retinal ganglion cells (ipRGCs), which are ganglion cells located in the retina that contain their own photoreceptors, including melanopsin. One role of these cells is to mediate circadian photoentrainment (Güler *et al.,* 2008). The decentralisation of circadian rhythm proteins found in fish indicates the potential for expression of this protein across a wide variety of tissues, which has been observed in zebrafish (Bellingham *et al.,* 2002). Melanopsin proteins found in teleost fish are divided into two main classes, with three mammalian-like and two *Xenopus*-like paralogs. The melanopsin proteins in the mammalian class include *opn4m1, opn4m2* and *opn4m3*. *Opn4m1* and *opn4m3* are characterised by their bistability, where the chromophore is retained in the opsin binding pocket during conversion between its *cis* and all *trans* configurations upon light stimulus. They are sensitive to wavelengths of light in the 470 - 484 nm range (Davies *et al.,* 2011). The other class is the *Xenopus*-like class and includes *opn4x1* and *opn4x2*. These along with *opn4m2* are characterised by the hydrolysis of their respective chromophores after light excitation causes the chromophore to convert to its *trans* configuration. All are found across a wide variety of teleost fish and have been characterized in model organisms such as zebrafish (Davies *et al.,* 2011). Four out of the five melanopsin genes present in zebrafish have been found in the starry flounder transcriptome, the exception being *opn4m2* (Beaudry *et al.,* 2017) (Figure 2), however the starry flounder sequences included in this study were predicted sequences. Since the work of Beaudry *et al.* (2017), whole genome sequence data for the starry flounder has become available, but there has been no research published to date that confirms if an *opn4m2* sequence is present in this species.

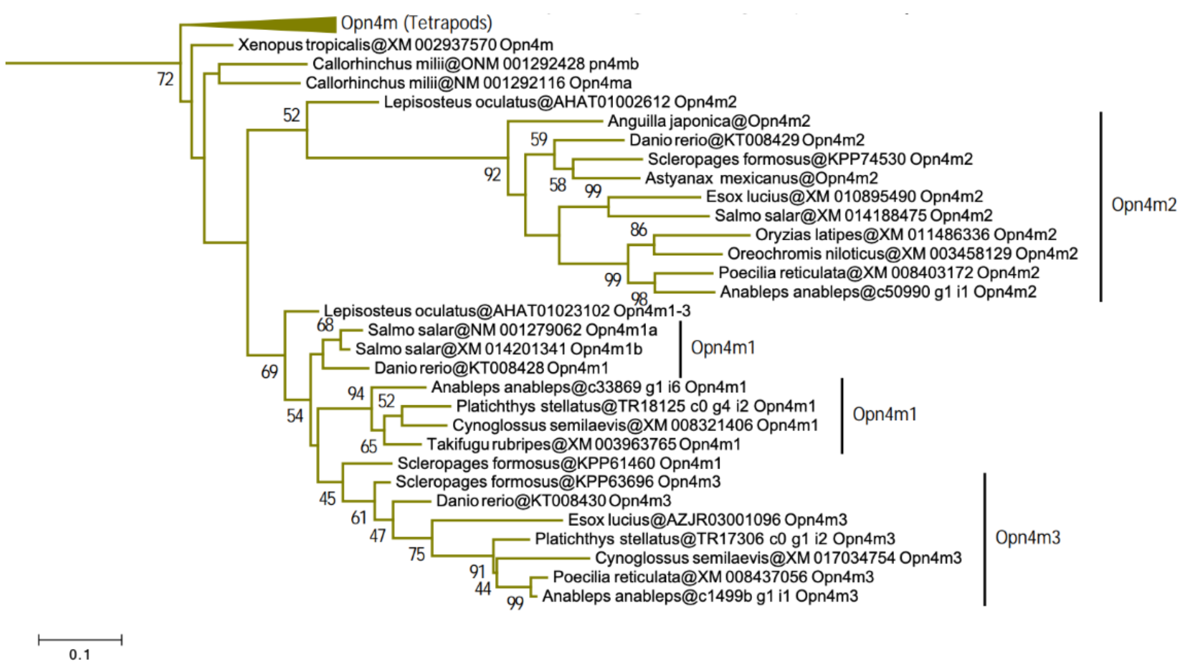

Figure 2. Phylogenetic tree of mammalian-like melanopsins in teleost fish. Tree courtesy of Beaudry *et al.* (2017).

These proteins as well as other non-visual opsins have the potential to make various organs light sensitive, however their functions in sensory systems remain to be fully investigated.

Starry flounder ecology

Starry flounder live primarily in shallow water. Their larval stage is mostly transparent and typically occupies shallow estuarine environments, meaning they are exposed to broad spectrum light throughout their early development (Bergstrom, 2007). Starry flounder are one of seven flatfish species found in the wild in both sinistral (Left-sided) and dextral (right-sided) morphs, meaning either the left or right side of the larvae becomes the top of the adult individual after metamorphosis is complete. This dimorphism is also observed to have a geographic cline leading to a 50:50 distribution of left sided and right sided individuals along the west coast of California and British Columbia and fully left sided populations along the coast of Japan. This polymorphism has been shown to be maintained in starry flounder populations around the Pacific Northwest and has been tied to several ecologically important factors (Bergstrom *et al.,* 2007). Bergstrom (2007) observed differences in the caudal peduncle and gill rakers between left and right sided individuals in populations from Victoria BC, however they found no significant difference in skull morphology. Additionally, that study found that the morphological differences were greater in populations where both morphs were represented equally (Bergstrom, 2007). While the genetics and ecological pressures surrounding the determination of sidedness remains unclear, the growing aquaculture of this species is leading to increased interest in these factors to determine the best culturing practices. Since the fisheries that are cultivating this species are primarily located in Asia, their populations are composed of almost entirely left sided morphs. While these hatcheries do end up with right sided morphs in their population, they are considered undesirable and do not have as high of a commercial value. Cultured individuals from Japanese populations also tend to have more right sided individuals in a laboratory setting than found in the wild, at roughly 13%. These factors are leading to increased research into sidedness and pigmentation that were not previously examined in a genetic context (Kang *et al.,* 2012).

Immunohistochemistry

A common technique for investigating expression of proteins in neural structures is the use of immunohistochemical staining, which uses fluorescently tagged antibodies to identify regions of protein expression in thin sections of tissue. In this experiment we were primarily interested in investigating the presence or absence of melanopsin, with a focus on qualitative assessment of differences between hemispheres rather than the amount of expression. Melanopsin mRNA has been detected in fish (zebrafish, Japanese flounder, and salmon) brains (Bellingham *et al.,* 2002; Liu *et al.,* 2020; Sandbakken *et al.,* 2012) but protein level investigations generally have not been done. Several antibodies were used in this study including GFAP, which labels radial glia cells (radial astrocytes) that act as both neural stem cells and scaffold cells during neural development. Melanopsin antibodies (immunolabels) used included OPN4L, which labels the melanopsin paralog *opn4m2* and pas350 which labels all mammalian-like melanopsin paralogs (*opn4m1, opn4m2,* and *opn4m3*). Tissues were also treated with the fluorescent nuclei stain DAPI to locate nuclei, which were used for identifying subregions of the optic tectum and to evaluate the quality of the tissue sections even if antibodies failed to bind.

Study design and hypothesis

This experiment involved using three left sided and three right sided flatfish to produce a thorough investigation of the impacts of sidedness on melanopsin expression. Fish were collected from Willows Beach in Victoria BC, on November 16th 2025 and on March 1st 2026, with fish of each sidedness collected on both sampling days. Immunolabelling of GFAP and melanopsins were done for at least two sections per fish, with images of one section from each fish being presented in this text. If opsins present in the brains of fish are light sensors, we would expect that they would be present in a way that is related to the amount of light stimulus a given area of the brain is exposed to. Because of this it is expected that there would be uneven expression of any proteins using this stimulus for behavioral or metabolic function. In a species like the starry flounder where light stimulus is not distributed evenly across the brain, we aimed to test the hypothesis that opsins are expressed to a greater extent on the side of the brain that intercepts light first, which differs between left and right sided morphs. The presence of both morphs in starry flounder populations found in the same area allows for an investigation into this expression in a way that is related to the sidedness of the individual rather than the sidedness of the species as a whole.

Previous experiments regarding melanopsin expression have not characterised it in the brains of the starry flounder. This study strives to fill that gap by qualitatively investigating melanopsin expression in the brains of these organisms and determining if there are any unusual patterns of expression that could potentially be linked to the sidedness of the individual. Further studies will be required to investigate the specific mechanisms of these proteins and establish more precise quantitative differences, however this experiment provided a baseline assessment of their presence and organisation to be used for future research, as well as an insight into starry flounder neuroanatomy.

Materials and Methods

Dissections

Prior to sampling, multiple starry flounder dissections were conducted using frozen samples from previous research to locate the brain and confirm the orientation of the optic tectum. The first dissection performed resulted in the optic tectum being located but orientation was lost. A second attempt at locating the optic tectum was unsuccessful. A dissection performed on the larger flatfish *Hippoglossus stenolepis* (Pacific Halibut) using a head discarded by local recreational fishers resulted in identifying regions of the skull to use to locate the brain. A third dissection of a starry flounder resulted in successful location of the brain.

Antibody tests

Sections of retina from zebrafish *(Danio rerio)* obtained from collaborators were used to assess the optimal concentrations for OPN4L and GFAP labelling following the immunolabelling protocol (Appendix A). Sections were treated with a blocking buffer (1X PBS with 2% goat serum). Primary antibody OPN4L was tested at dilutions of 1:500 and 1:250 (diluted in 1X PBS, rabbit anti-*opn4m2* polyclonal antibody, invitrogen Cat. No. PA5-72273 Lot No. 79560889). Primary antibody GFAP was tested at dilutions of 1:1600, 1:1000, and 1:2000 (diluted in 1X PBS, chicken anti-GFAP polyclonal antibody, invitrogen Cat. No. PA1-10004 Lot No. XI3685001 mixed 1:1 with glycerol). Secondary antibodies were Alexa 555 (diluted 1:500 in 1X PBS, AlexaFluor^{TM} 555 donkey anti-rabbit lgG (H+L) 2 mg/mL, Invitrogen Cat. No. A31572 Lot No. 2339822) and Alexa 488 (diluted 1:500 in 1X PBS, AlexaFluor^{TM} 488 goat anti-chicken lgY(H+L) 2 mg/ml, Invitrogen Cat. No. A11039 Lot. No. 2420700 mixed 1:1 with glycerol). Slides were mounted with a mounting medium containing DAPI (DAPI Fluoromount-G™, Electron Microscopy Sciences Cat. No. 17984-24 Lot No. 230207)) and sealed with clear nail polish. Slides were then left overnight to incubate at 4º C. Slides were imaged using a confocal microscope (a Nikon C2, using the 20x (numerical aperture 0.75) objective lens). Image processing was done using FIJI (Fiji Is Just ImageJ version 1.54p, Java 1.8.0_322 (64-bit) with BioVoxxel: Figures Tools version 4.1.0 https://doi.org/10.5281/zenodo.14217141).

Sampling

Animals used in this experiment were collected with approval from the UVic animal care committee (AUP) #AE-25-013. Sampling was conducted with permission from fisheries and oceans Canada (DFO) scientific licence to fish #XR 508 2025. An overview of all the fish samples in this study and how they were used are presented in Table 1.

Table 1. Overview of samples used in this experiment.

Species	Count	Use
Zebrafish (*Danio rerio*)	1 retina	6 sections were labeled to assess concentrations of OPN4L antibody
Starry flounder (*Platichthys stellatus*) (frozen)	3	3 starry flounder frozen from previous research were used for preliminary dissections; no sectioning or labelling was done on these samples.
Halibut (*Hippoglossus stenolepis*)	1 head	Preliminary dissection was done using discarded head; no sectioning or labelling was done on these samples
Starry flounder (*Platichthys stellatus*)	11 total	11 starry flounder were caught and euthanised in total. Of these, 10 received cryoprotection and embedding in OCT (one was left in PBS). Of these, 8 were sectioned while 2 remained frozen in OCT. Of these, 6 were labelled with either OPN4L or pas350 while one was used for an optic nerve label and one did not receive labelling.

The first round of sampling was done at Willows Beach in Victoria BC beginning at 8:44 am on November 16, 2025. A beach seine was used four times. The first seine at 9:00 am resulted in capture of two left sided individuals, the second and third seines at 9:20 am and 9:40 am respectively were unsuccessful. The fourth seine at 10:00 am resulted in capture of three individuals (2 left sided and 1 right sided). The tide was high (2.4m), and water temperature was 9º C. Fish were euthanised in a 2L tank containing 220mg/250mL of TMS (MS-222) following UVic fish euthanasia SOP (OA2003). Once euthanised, fish were measured for length from tip of snout to tail and heads were removed (Table B1.). A perforation was made along the top of the lateral line prior to fixation in 4% paraformaldehyde (PFA). Heads in PFA were stored in a fridge at 4º C overnight. The next day, additional dissections were performed to fully remove the brains for the right sided and three of the left sided samples, while one of the left sided samples had the brain exposed but eyes and skull remained. Samples were moved to fresh PFA and fixed for an additional 3 hours. Samples were then placed in a cryoprotectant solution (30 % sucrose in 1X PBS) and left overnight. The next day after they had sunk in the sucrose, samples were placed in a mix of 50% sucrose (30 % sucrose in 1X PBS) and 50% optimal cutting temperature compound (OCT) and left overnight. The following day samples were moved to 100% OCT and left overnight. Samples were removed from OCT and placed in molds with fresh OCT. Samples were then frozen in liquid nitrogen. The sample containing the eyes and skull was left an additional overnight in 100% OCT before being frozen in the sample tube using liquid nitrogen. Frozen samples were stored at -70º C.

The second round of sampling was done at Willows Beach in Victoria BC beginning at 8:50 am on March 1st 2026. A beach seine was used twice. The first seine at 9:00 am resulted in capture of 3 right sided individuals, a second seine at 9:30 resulted in capture of three individuals (2 right sided and one left sided). The tide was high (2.3m) and water temperature was 8.6º C. Fish were euthanised in a 2L tank containing 220mg/250mL of TMS (MS-222) following UVic fish euthanasia SOP (OA2003). Once euthanised, fish were measured for length from tip of snout to tail and heads were removed (Table B1.). Complete removal of the brain occurred directly after euthanasia and excised brains were placed immediately in 4% PFA. One right sided sample also had the eyes placed in PFA, but the eyes were not punctured. After 6 hours, samples were moved to 1X PBS. After 21 hours, samples were transferred from 1X PBS to 30% sucrose (30 % sucrose in 1X PBS) and left overnight. Samples were left for an additional overnight in 30% sucrose. Samples were then placed in 100% OCT and left overnight. One left sided sample had both the brain and eyes fixed and was left an additional overnight in 30% sucrose. That sample was moved to 100% OCT the following morning. Samples were stored in OCT at 4º C. Samples were embedded and frozen on the day of sectioning using dry ice.

Sectioning

Sectioning of a left sided individual from the first round of sampling was done on November 25th 2025 (five days after embedding). Sectioning was performed to a thickness of 20µm using Leica Cryostat (Leica CM1850UV). Samples were collected using adhesive slides (NewSilane Adhesive Coated Slides, White Frosted, Newcomer Supply Cat. No. 5070). Sectioning of a right sided individual from the first round of sampling was done to a thickness of 20 µm on January 13th 2026 (54 days after embedding). Sectioning of a left sided individual from the first round of sampling was done to a thickness of 40 µm on January 21st 2026 (62 days after embedding). Sectioning of two right sided and one left sided individual from the second round of sampling were done to a thickness of 40µm (day of embedding).

Optic nerve labelling

Two starry flounder caught in March 2026 were euthanised following the previously described protocol. Prior to sectioning, Alexa Fluor 647 conjugated to 10 000 MW dextran (10% weight/volume in 2% DMSO) was applied to the end of the optic nerve of one fish. This was then incubated at room temperature in bubbled (5% CO_2 and 95% O_2) amphibian artificial cerebrospinal fluid (ACSF) for 6 hours. This was then left overnight at 6º C in the ACSF. The sample was then fixed in 4% PFA for 6 hours. The sample was stored for six days at 4ºC in 1X PBS. The previous steps were completed by collaborators. The sample was transferred from 1X PBS to 30% sucrose (30 % sucrose in 1X PBS) and left for two days. Sample was then placed in 100% OCT and left overnight. The sample was sectioned to a thickness of 40 µm on the day of embedding.

Immunolabelling:

There were around 30 sections obtained for each brain, and of these the best slide (set of three sections) was chosen for each fish and labelled. Of these, the two best sections were chosen for primary antibody labelling and the worst was selected as the no primary antibody added control. Both labelled sections from each fish were imaged and the better of the two was selected for inclusion in this manuscript. Sections were assessed for quality based on the number and length of tears in the tissue, specifically the optic tectum. After imaging, the optic tectum was examined for clarity of labelling and lack of small tears. The best part of each optic tectum hemisphere from the same brain was selected for the final close-up images. Antibodies used and their concentrations are detailed in the table below (Table 2).

Table 2. Overview of antibodies used in this experiment.

Antibody	Protein(s) detected	Host species	Dilution used unless otherwise specified
OPN4L	*Opn4m2*	Rabbit	1:1000
Pas350	*Opn4m1, opn4m2,* and *opn4m3.*	Rabbit	1:500
GFAP	Glial fibrillary acidic protein	chicken	1:1600
Alexa 488	GFAP primary antibody	Goat	1:500
Alexa 555	OPN4L and pas350 primary antibodies	donkey	1:500

Sections from the left sided individual sectioned on November 25th were labelled following the immunolabelling protocol (Appendix A) with an extra 13 minutes added to the blocking buffer incubation time. Primary antibodies used were OPN4L (diluted 1:500 in 1X PBS) and GFAP Secondary antibodies were Alexa 555 and Alexa 488. Labelling from this section was assessed for clarity. Because of this, a dilution of 1:1000 for OPN4L and Alexa 555 was used for the next sample. All subsequent samples used a 1:1000 dilution for OPN4L and Alexa 555 as this provided clearer results.

Sections from the right sided individual sectioned on January 13th, as well as sections from the two right sided individuals and one left sided individual from the second round of sampling were labelled following the immunolabelling protocol (Appendix A). Primary antibodies used were OPN4L and GFAP, Secondary antibodies were Alexa 555 and Alexa 488.

Sections from the left sided individual sectioned on January 21st as well as a section from sablefish (*Anoplopoma fimbria*) from collaborators were labelled following the immunolabelling protocol (Appendix A). Primary antibodies used were pas350 (gifted by Davies *et al* in 2021) and GFAP. Secondary antibodies were Alexa 555 and Alexa 488.

For all labelling, slides were mounted with a mounting medium containing DAPI and sealed with clear nail polish. Slides were then left overnight at 4º C.

Imaging

Slides were imaged using a Nikon C2 confocal microscope using the 20x (numerical aperture 0.75) objective lens. Images were taken in three channels, 405 nm laser for DAPI, 488 nm laser for Alexa 488, and 561 nm laser for Alexa 555. For the samples with the optic nerve label, they were imaged using the 405 nm and 640 nm lasers. Image processing was done using FIJI. Imaging settings for each sample are detailed in Table B2.

Results

Dissections

Dissections done prior to the experiment confirmed that the sideways brain orientation found in flatfish was present in this species, as well as provided practice and identification of brain structures for analysis of final labelling images (Figure 3).

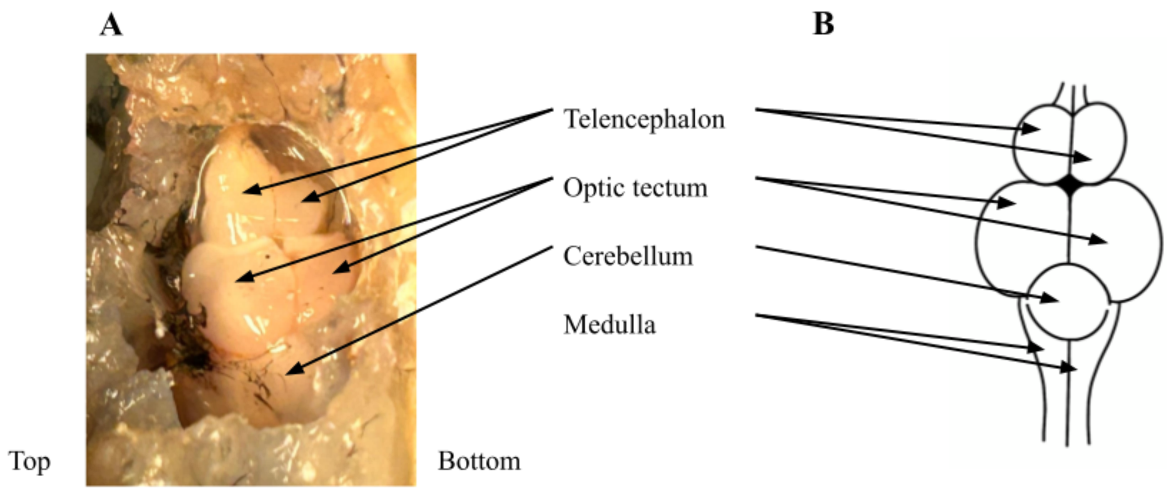

Figure 3. Brain of *Platichthys stellatus* labelled with telencephalon, optic tectum, cerebellum, and medulla. (A) Image taken of a left sided individual from the third preliminary dissection. Top (eyed) side and bottom (blind) side of the fish are indicated. The medulla is not visible in the image. (B) Diagram of the brain drawn using procreate (version 5.3, Savage Interactive).

Antibody tests

First, several antibody concentrations were tested to identify a starting point for the antibody concentrations. Successful labelling of *Danio rerio* retina indicated the antibodies were working correctly (Figure 4). The dilutions of 1:500 for OPN4L and 1:1600 for GFAP primary antibodies were selected for the subsequent brain labelling as they provided the clearest results in the retinal sections. GFAP was used throughout the experiment as a marker of radial glia cells throughout the optic tectum as previous work in the lab has characterised their location in other fish species including sablefish and zebrafish (Mokariasl, 2024). There was clear labelling in the photoreceptor layer and the identification of amacrine cells, consistent with previous results. Labelling of a starry flounder retina resulted in identification of several retinal layers including labelling of Muller glia by GFAP and the inner and outer nuclear layers being seen with DAPI. There was some potential OPN4L labelling in the photoreceptor layer present (Figure 5). Successful labelling of sablefish optic tectum indicated the pas350 antibody was working correctly (Figure 6). Presence of striations and labelling of a neuronal subpopulation in the bottom of the periventricular grey area in this sample was consistent with previous work done in the lab (Mokaraisl, 2024). DAPI staining indicated the nuclei of neurons present and provided clear identification of the various brain layers such as the periventricular grey area and radial astrocyte nuclei.

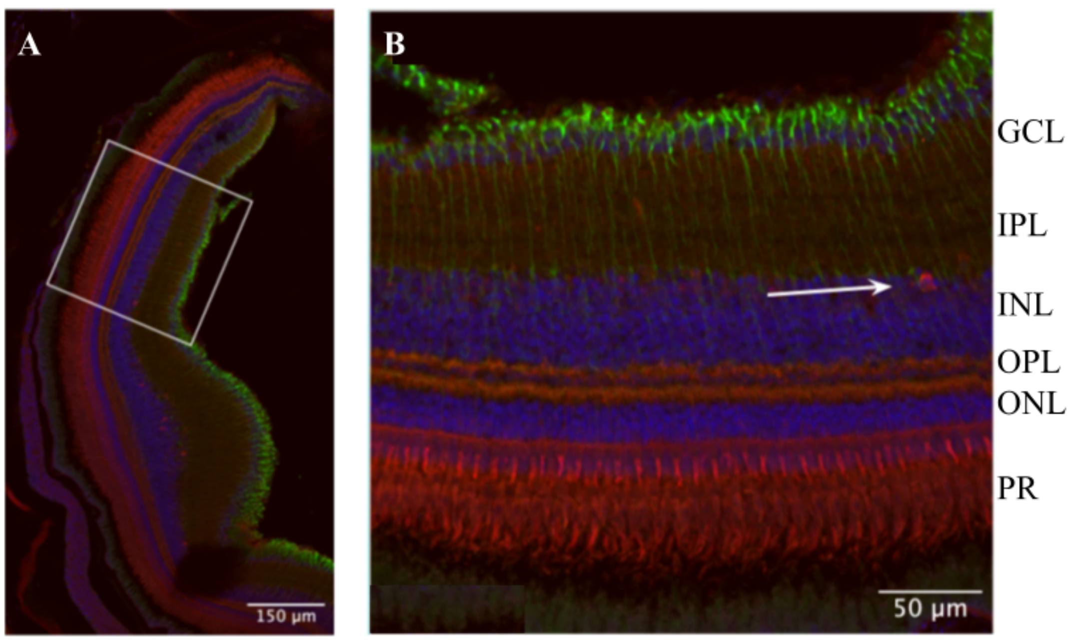

Figure 4. Immunofluorescent labeling of retina of *Danio rerio*. Red: Primary antibody OPN4L (diluted 1:500 in 1X PBS), secondary antibody was Alexa 555 (diluted 1:500 in 1X PBS). Green: Primary antibody GFAP (diluted 1:2000 in 1X PBS), secondary antibody was Alexa 488 (diluted 1:500 in 1X PBS). Blue: Nuclei counterstained with DAPI. (A) Composite image of whole retina, scale bar indicates 150µm. (B) Inset showing an OPN4L labelled amacrine cell labelled with an arrow, one of several throughout the sample. Scale bar indicates 50µm. GCL: ganglion cell

layer, IPL: inner plexiform layer, INL: inner nuclear layer, OPL: outer plexiform layer, ONL: outer nuclear layer, PR: photoreceptors.

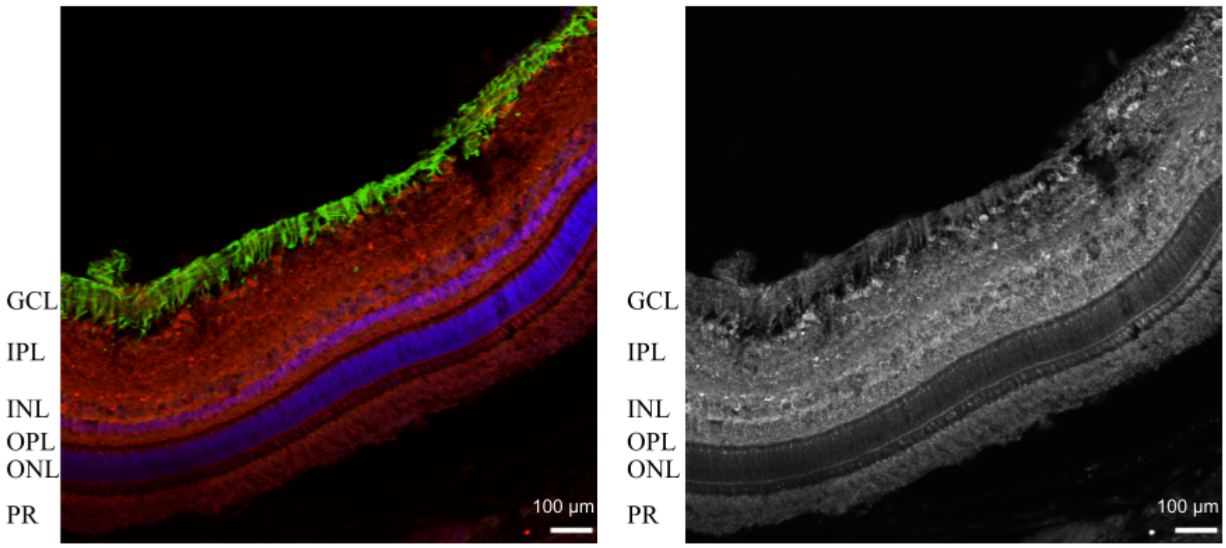

Figure 5. Immunofluorescent labeling of retina of right sided *Platichthys stellatus*. Red Primary antibody OPN4L (diluted 1:1000 in 1X PBS), secondary antibody was Alexa 555 (diluted 1:1000 in 1X PBS). Green: Primary antibody GFAP (diluted 1:1600 in 1X PBS), secondary antibody was Alexa 488 (diluted 1:500 in 1X PBS). Blue: Nuclei counterstained with DAPI. Scale bars represent 100 µm. GCL: ganglion cell layer, IPL: inner plexiform layer, INL: inner nuclear layer, OPL: outer plexiform layer, ONL: outer nuclear layer, PR: photoreceptors. (A) Composite image with all colour channels. (B) Greyscale of OPN4L labelling only.

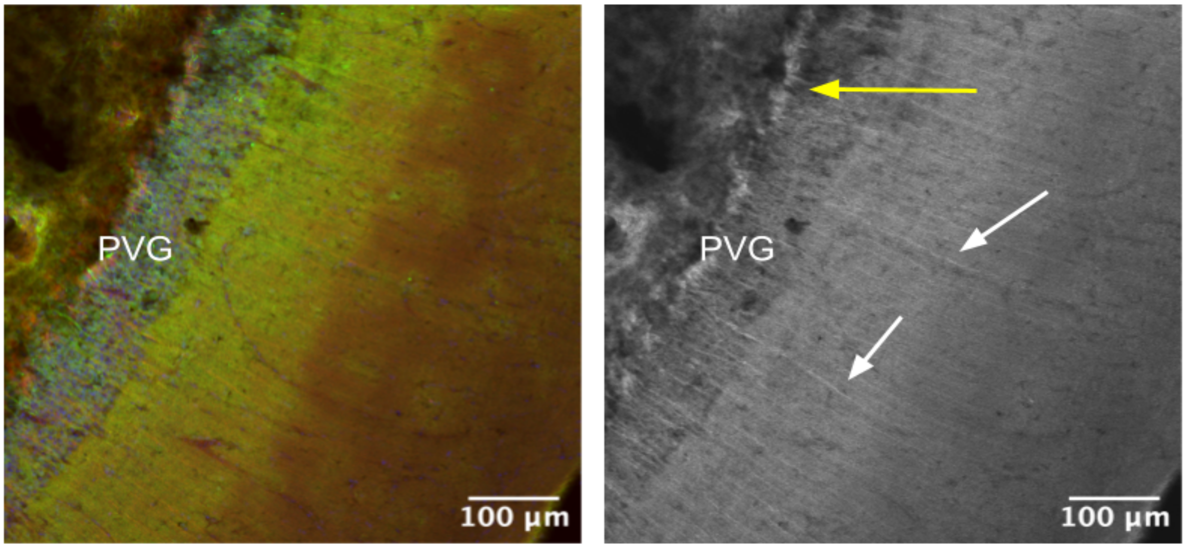

Figure 6. Immunofluorescent labeling of optic tectum of *Anoplopoma fimbria*. Red: Primary antibody pas350 (diluted 1:500 in 1X PBS), secondary antibody was Alexa 555 (diluted 1:1000 in 1X PBS). Green: Primary antibody GFAP (diluted 1:1600 in 1X PBS), secondary antibody was Alexa 488 (diluted 1:500 in 1X PBS). Blue: Nuclei counterstained with DAPI. Scale bars represent 100µm. PVG: periventricular grey. (A) Composite image. (B) Greyscale of pas350 labelling only. The yellow arrow indicates neurons labelled near the bottom of the periventricular grey area. White arrows indicate labelling in radial astrocytes.

Starry flounder immunolabelling

After antibodies were determined to be working and brain orientation was confirmed, melanopsin and GFAP expression could be investigated in the starry flounder brains. Immunolabelling of starry flounder brains resulted in identification of several regions of labelling including the optic tectum. Other regions also showed potential labelling with some samples showing labelling throughout the hypothalamus and medulla regions (Figure 7). Presence of labelled cells in the optic tectum of sections labelled with OPN4L was seen in both left and right sided samples (Figures 7 - 12). Some of these regions also had overlapping labelling in the green channel, but it was not as bright and only noted in the sample labelled with a 1:500 dilution of primary antibody OPN4L (Figure 11). These were indistinguishable from blood vessels in the sample labelled with pas350 (Figure 13). All OPN4L labelled samples also showed labelling in the periventricular grey area (Figure 7-12).

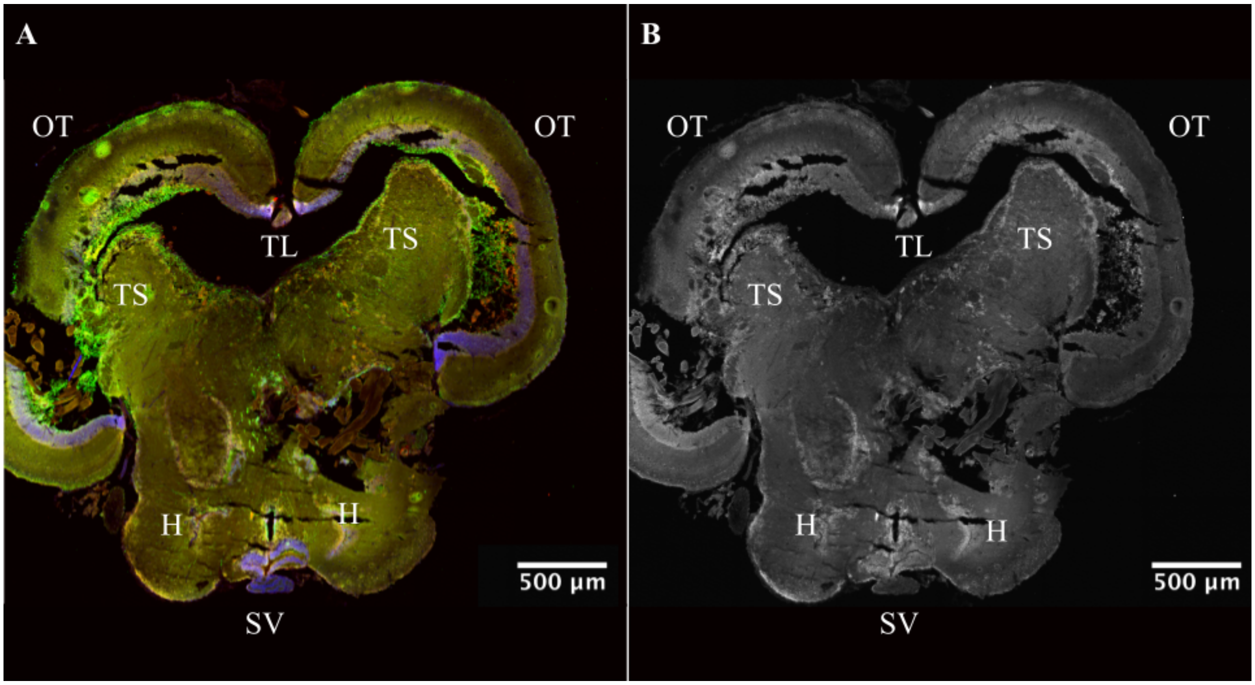

Figure 7. Immunofluorescent labeling of the whole brain of right sided *Platichthys stellatus* from first round of sampling. Red: Primary antibody OPN4L (diluted 1:1000 in 1X PBS), secondary antibody was Alexa 555 (diluted 1:1000 in 1X PBS). Green: primary antibody GFAP (diluted 1:1600 in 1X PBS), secondary antibody was Alexa 488 (diluted 1:500 in 1X PBS). Blue: Nuclei counterstained with DAPI. Scale bar indicates 500µm. OT: optic tectum, TS: torus semicircularis, TL: torus longitudinalis, H: hypothalamus, SV: saccus vasculosus. (A) Composite image. (B) Greyscale of OPN4L labelling only.

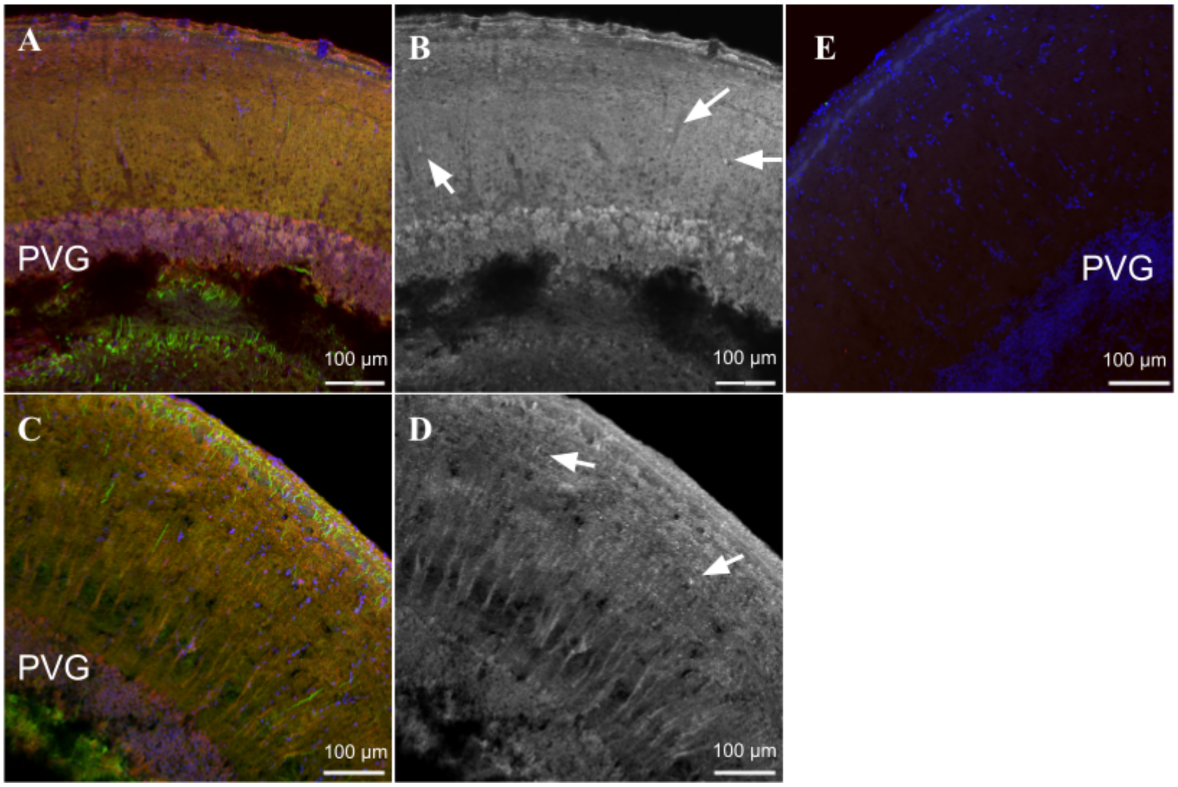

Figure 8. Immunofluorescent labeling of optic tectum of right sided *Platichthys stellatus* from the second round of sampling. Red: Primary antibody OPN4L (diluted 1:1000 in 1X PBS), secondary antibody was Alexa 555 (diluted 1:1000 in 1X PBS). Green: Primary antibody GFAP (diluted 1:1600 in 1X PBS), secondary antibody was Alexa 488 (diluted 1:500 in 1X PBS). Blue: Nuclei counterstained with DAPI. Scale bars represent 100 μm. PVG: periventricular grey area. (A) Composite image of the upward facing right hemisphere of the optic tectum. (B) Greyscale of OPN4L labelling only in image A. Arrows indicate cells labelled by OPN4L. (C) Composite image of the downward facing left hemisphere of the optic tectum. (D) Greyscale of OPN4L labelling only in image C. Arrows indicate cells labelled by OPN4L. (E) Control image with no primary antibody added showing all colour channels.

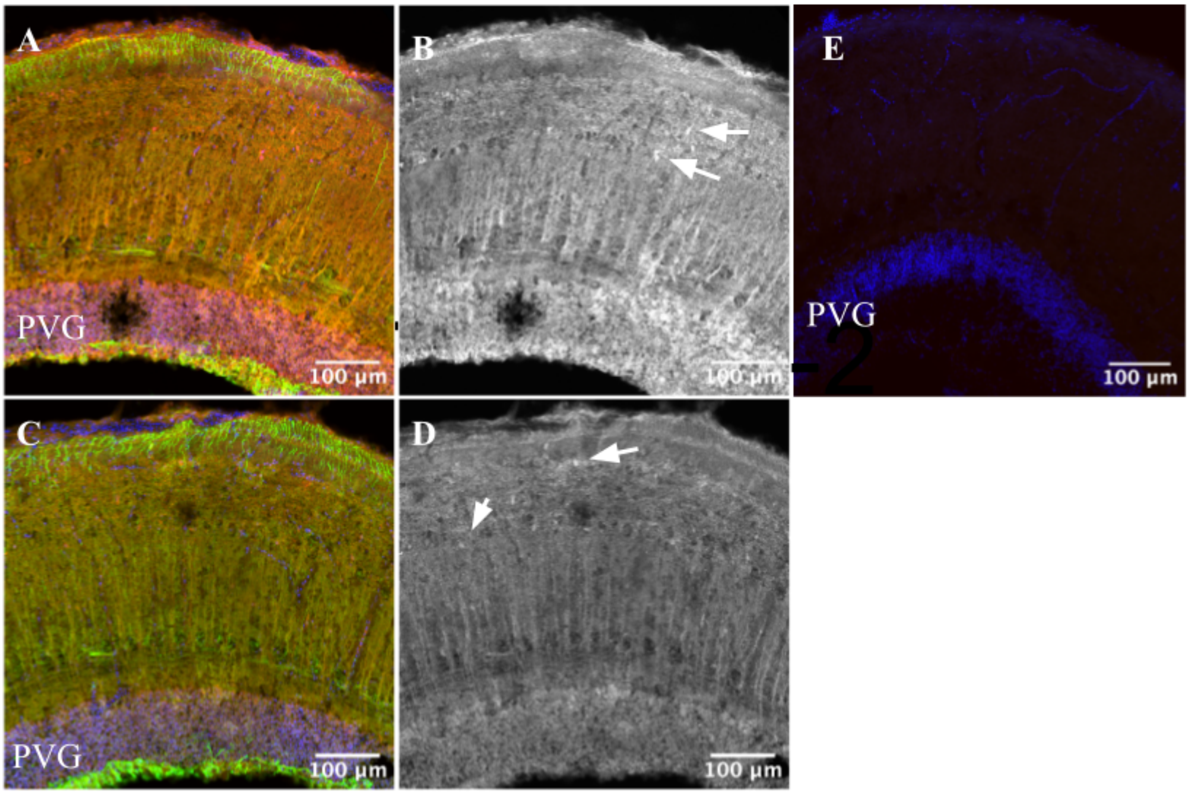

Figure 9. Immunofluorescent labeling of optic tectum of right sided *Platichthys stellatus* from the second round of sampling. Red: Primary antibody OPN4L (diluted 1:1000 in 1X PBS), secondary antibody was Alexa 555 (diluted 1:1000 in 1X PBS). Green: Primary antibody GFAP (diluted 1:1600 in 1X PBS), secondary antibody was Alexa 488 (diluted 1:500 in 1X PBS). Blue: Nuclei counterstained with DAPI. Scale bars represent 100 µm. PVG: periventricular grey area. (A) Composite image of the downward facing left hemisphere of the optic tectum. (B) Greyscale of OPN4L labelling only in image A. Arrows indicate cells labelled by OPN4L. (C) Composite image of the upward facing right hemisphere of the optic tectum. (D) Greyscale of OPN4L labelling only in image C. Arrows indicate cells labelled by OPN4L. (E) Control image with no primary antibody added showing all colour channels.

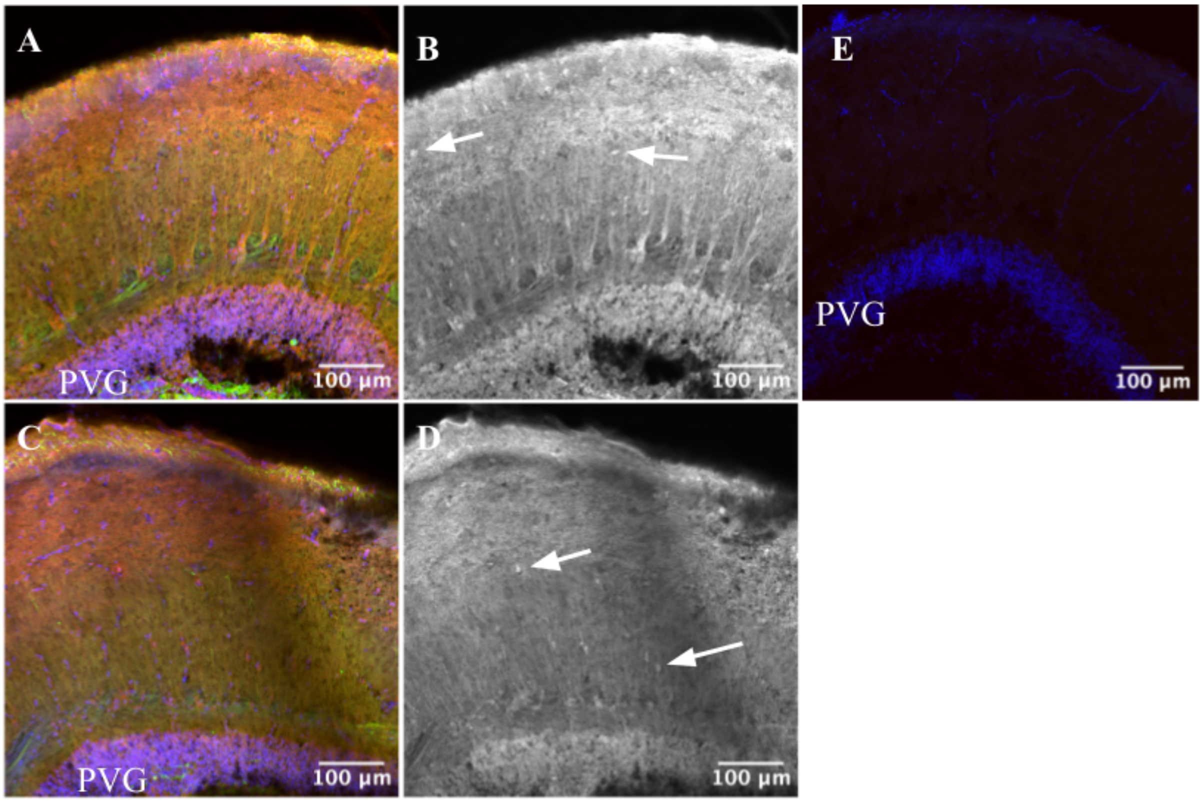

Figure 10. Immunofluorescent labeling of optic tectum of left sided *Platichthys stellatus* from the second round of sampling. Red: Primary antibody OPN4L (diluted 1:1000 in 1X PBS), secondary antibody was Alexa 555 (diluted 1:1000 in 1X PBS). Green: Primary antibody GFAP (diluted 1:1600 in 1X PBS), secondary antibody was Alexa 488 (diluted 1:500 in 1X PBS). Blue: Nuclei counterstained with DAPI. Scale bars represent 100 µm. PVG: periventricular grey area. (A) Composite image of the downward facing right hemisphere of the optic tectum. (B) Greyscale of OPN4L labelling only in image A. Arrows indicate cells labelled by OPN4L. (C) Composite image of the upward facing left hemisphere of the optic tectum. (D) Greyscale of OPN4L labelling only in image C. Arrows indicate cells labelled by OPN4L. (E) Control image with no primary antibody added showing all colour channels.

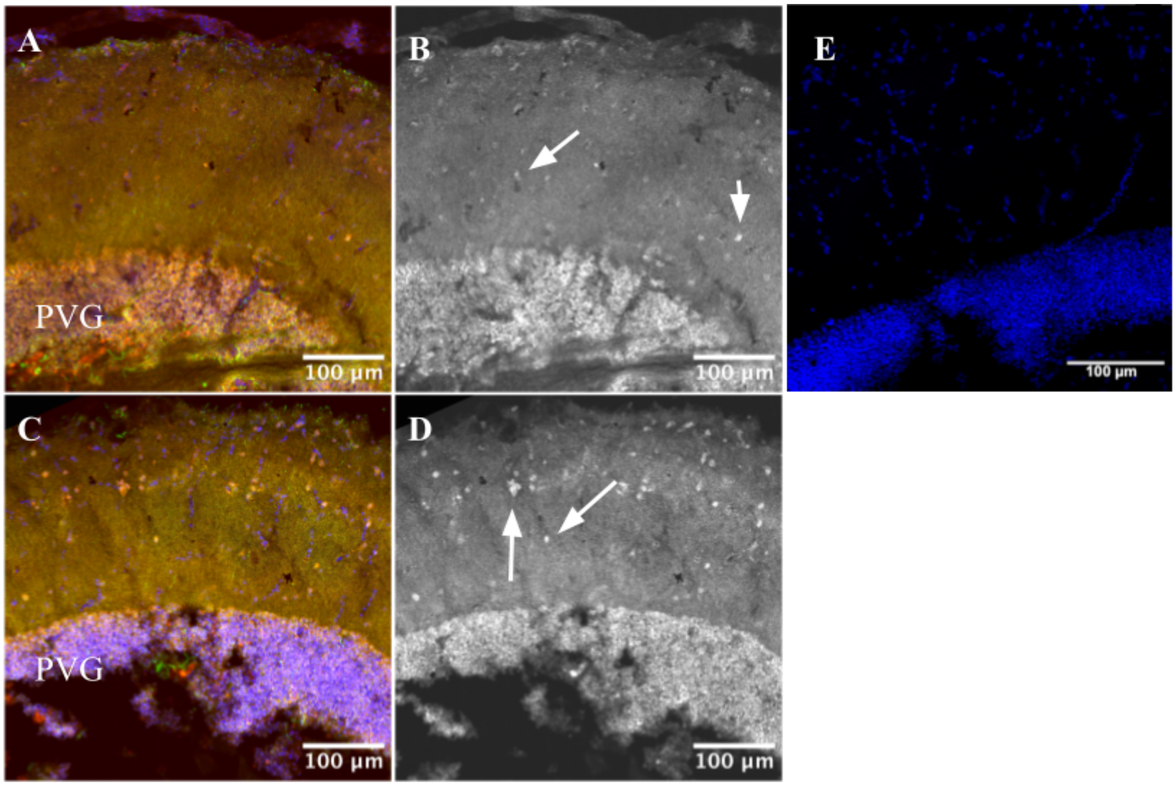

Figure 11. Immunofluorescent labeling of optic tectum of left sided *Platichthys stellatus* from first round of sampling. Red: Primary antibody OPN4L (diluted 1:500 in 1X PBS), secondary antibody was Alexa 555 (diluted 1:500 in 1X PBS). Green: Primary antibody GFAP (diluted 1:1600 in 1X PBS), secondary antibody was Alexa 488 (diluted 1:500 in 1X PBS). Blue: Nuclei counterstained with DAPI. Scale bars represent 100µm. PVG: periventricular grey area. (A) Composite image of the upward facing left hemisphere of the optic tectum. (B) Greyscale of OPN4L labelling only in image A. Arrows indicate cells labelled by OPN4L. (C) Composite image of the downward facing right hemisphere of the optic tectum. (D) Greyscale of OPN4L labelling only in image C. Arrows indicate cells labelled by OPN4L. (E) Control image with no primary antibody added showing all colour channels.

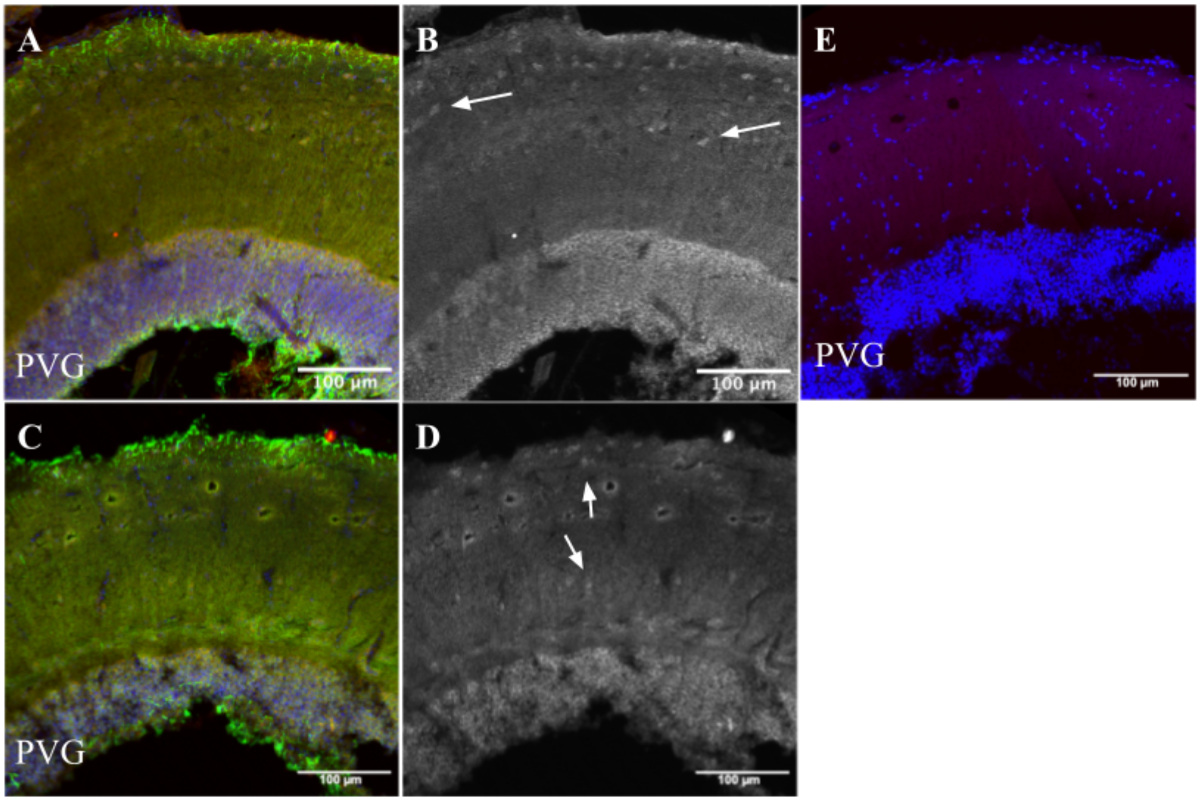

Figure 12. Immunofluorescent labeling of optic tectum of right sided *Platichthys stellatus* from first round of sampling. Red: Primary antibody OPN4L (diluted 1:1000 in 1X PBS), secondary antibody was Alexa 555 (diluted 1:1000 in 1X PBS). Green: primary antibody GFAP (diluted 1:1600 in 1X PBS), secondary antibody was Alexa 488 (diluted 1:500 in 1X PBS). Blue: Nuclei counterstained with DAPI. Scale bars indicate 100µm. PVG: periventricular grey area. (A) Composite image of the upward facing right hemisphere of the optic tectum. (B) Greyscale of OPN4L labelling only in image A. Arrows indicate cells labelled by OPN4L. (C) Composite image of the downward facing left hemisphere of the optic tectum. (D) Greyscale of OPN4L labelling only in image C. Arrows indicate cells labelled by OPN4L. (E) control image of the right hemisphere of the optic tectum with no primary antibody added showing all colour channels.

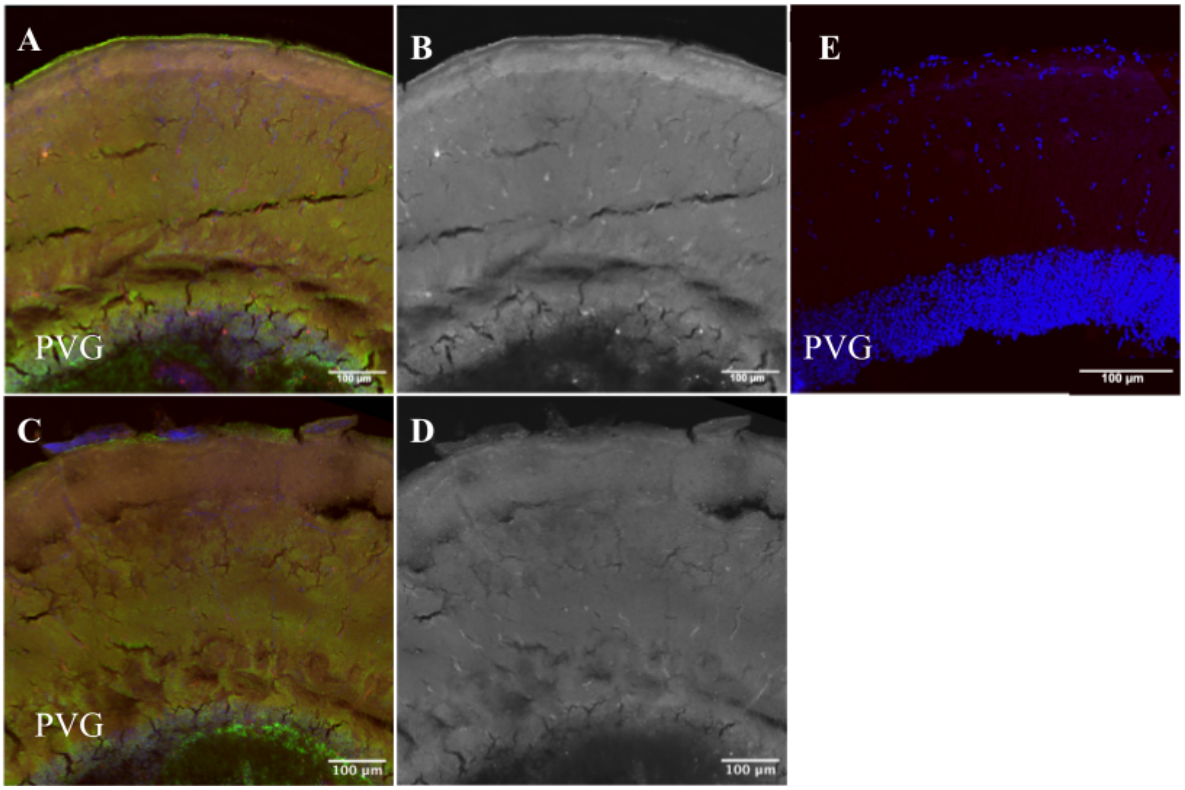

Figure 13. Immunofluorescent labeling of optic tectum of left sided *Platichthys stellatus* from first round of sampling. Red: Primary antibody pas350 (diluted 1:500 in 1X PBS), secondary antibody was Alexa 555 (diluted 1:1000 in 1X PBS). Green: Primary antibody GFAP (diluted 1:1600 in 1X PBS), secondary antibody was Alexa 488 (diluted 1:500 in 1X PBS). Blue: Nuclei counterstained with DAPI. Scale bars represent 100 µm. (A) Composite image of the upward facing left hemisphere of the optic tectum. (B) Greyscale of pas350 labelling only in image A. Arrows indicate cells labelled by OPN4L. (C) Composite image of the downward facing right hemisphere of the optic tectum. (D) greyscale of pas350 labelling only in image C. Arrows indicate cells labelled by OPN4L. (E) Control image with no primary antibody added showing all colour channels.

Additional labelling

Notably, the blood vessel labelling was only present in the pas350 sample. This was clear blood vessel labelling as determined by observation of DAPI staining patterns, this labeling was not present in the samples labelled with OPN4L (Figure 14).

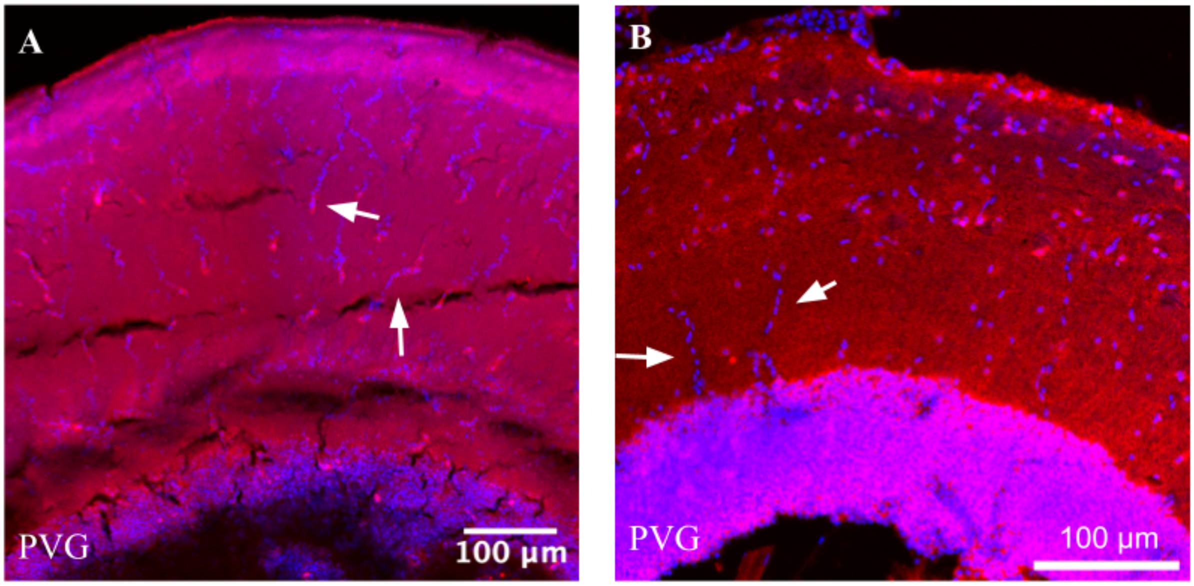

Figure 14. Immunofluorescent labeling of optic tectum sections of *Platichthys stellatus* from the first round of sampling. Blue: Nuclei counterstained with DAPI. Scale bars indicate 100µm. The brightness was raised post-imaging using FIJI image software to increase visibility of the red channel against the black background. (A) Close up of the upward facing left hemisphere of the optic tectum in the left sided individual shown in figure 13. Red: Primary antibody pas350 (diluted 1:500 in 1X PBS), secondary antibody was Alexa 555 (diluted 1:1000 in 1X PBS). Arrows indicate blood vessels as identified using DAPI nuclei stain patterns with labelling by the pas350 antibody. (B) Close up of the downward facing left hemisphere of the right sided individual shown in figures 7 and 12. Red: Primary antibody OPN4L (diluted 1:1000 in 1X PBS), secondary antibody was Alexa 555 (diluted 1:1000 in 1X PBS). Arrows indicate blood vessels as identified using DAPI nuclei stain patterns.

Optic nerve labelling of a starry flounder brain resulted in no clear fluorescent labelling. Fluorescence was present in sample mounted with DAPI that had the optic nerve label applied to one optic nerve prior to sectioning, however it appeared across the tissue (Figure 15).

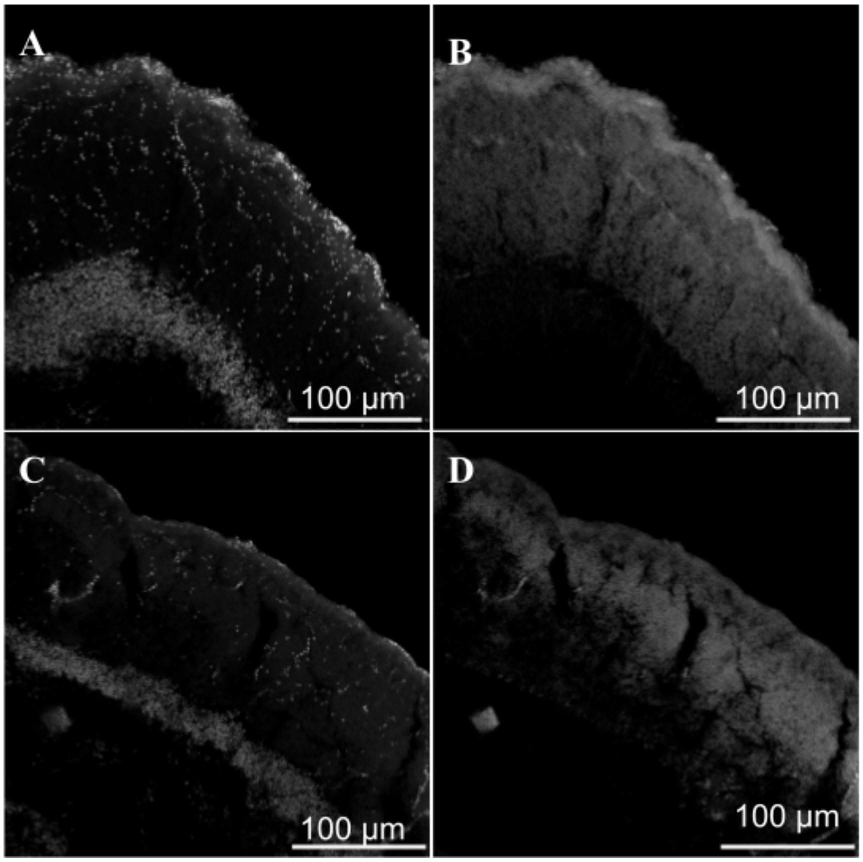

Figure 15. Immunofluorescent image of optic tectum of right sided *Platichthys stellatus* from the second round of sampling. Tissue was labelled with an optic nerve label applied to severed optic nerves before sectioning. Scale bars represent 100 µm. (A) Downward facing left hemisphere of optic tectum imaged with 405 nm laser. (B) Downward facing left hemisphere of optic tectum imaged with 640 nm laser. (C) Upward facing right hemisphere of optic tectum imaged with 405 nm laser. (D) Upward facing right hemisphere of optic tectum imaged with 640 nm laser.

Discussion

The purpose of this experiment was to investigate expression of melanopsin in starry flounder brains. This was done specifically for the melanopsin *opn4m2*. Clear results of labelling done with *D. rerio* retinal sections indicated that the OPN4L primary antibody used in this experiment was working properly. Melanopsin labeling is known to be present in the photoreceptor layer as well as the interneurons for retinal ganglion cells (amacrine cells) (Bailes and Lucas, 2009). There was also clear labelling by GFAP in the radial astrocytes which is as expected and indicated this antibody was working. Labelling of sablefish optic tectum with pas350 indicated that the pas350 antibody was also working properly. The sablefish section labelled in this study had some labelling visible across the top of the optic tectum and displayed the pas350 labelling being localised to the bottom of the periventricular grey zone, consistent with the results from a previous PhD student in the lab (Mokariasl, 2024). The confirmation of correctly working antibodies indicates that there were no issues with the antibodies themselves.

Starry flounder whole genome data is still largely unannotated. Whole genome sequencing of the species was only done recently in relation to this study so work may be being done currently to annotate the genome (Zheng *et al.,* 2025). Because of this, confirmation that these fish do indeed have a homologous *opn4m2* sequence could not be done using starry flounder sequence data. Additionally, the study by Beaudry *et al.* (2017) was unable to identify a starry flounder *opn4m2* sequence. Genome searching found an *opn4m2* sequence in *H. stenolepis*. The presence of *opn4m2* has also been shown in *Paralichthys olivaceous* (Liu *et al.,* 2020), although this study notes that it has multiple exons which is inconsistent with previous research that suggests *opn4m2* arose from a retrotransposition event and is subsequently intronless (Davies *et al.,* 2011). Although not commented on by Liu *et al.* (2020), their methods of mining the *P. olivaceous* genome to find these sequences and the alignment programs used for exon structure determination may have caused this. The presence of this sequence in the closely related species *P. olivaceous*, indicates it is very likely that this protein is present in the starry flounder.

Retina

While the starry flounder retina labelling looked very different from the giant danio labelling, identification of retinal ganglion receptor layers as well as the nuclear layers was still possible. There was labelling of photoreceptors by OPN4L, but it was less clear than in the giant danio. The inclusion of a retina was not the focus of this study and subsequently the sections used for labelling were not chosen based on retina quality but on the quality of the brains that were included in the section. Additionally, the fixation procedure used was one that had been optimised for brain tissue and was likely not optimal for retinal tissue. Despite this there was still presence of the expected nuclear layers in DAPI and the GFAP layer, they were just not as well defined. The photoreceptor layer appears to be present, but there were no cells present that could be confidently identified as amacrine cells present. While incorrect fixation of the tissue could have led to non-specific binding of the OPN4L antibody, the presence of the expected layers suggests potential melanopsin presence in the retina. The previously mentioned role of melanopsin and its presence in ipRGCs suggests that this is a region where labelling should be present. Additionally, if there is higher expression of *opn4m2* in the retina than the brain for the starry flounder as there is in the Japanese flounder (Liu *et al.,* 2020), using the same concentrations of antibodies as the brain could result in a brighter signal. Overall, the labelling in the retina is where it is expected to be based on the results from the *Danio* labelling, the tissue itself just appears to be incorrectly fixed.

Optic tectum labelling

Labelling with OPN4L resulted in small cells in the optic tectum being labelled. These were also potentially present in the samples labelled with pas350, but they could not be distinguished from the blood vessels. These cells looked like labelled interneurons. They were observed across the entire optic tectum in most samples in a random manner. These along with the labelling in the periventricular grey area indicate the presence of a large number of neurons being labelled by the OPN4L antibody rather than a subpopulation as was seen in the sablefish (Mokariasl, 2024). These results look very similar to an immunohistochemical study of the fish optic tectum performed by Lindsey *et al.* (2019) where the monoclonal antibody HuC/D was used to fluorescently label all the neurons in a coronal section of tissue. HuC/D is a pan-neuronal marker that labels the RNA binding proteins HuC and HuD and shows where the cell bodies of neurons are located. These labelling patterns lead to bright labelling in the periventricular grey area where many of the neuronal cell bodies are located, as well as sporadic single cell labeling of interneurons scattered throughout the upper portions of the optic tectum (Lindsey *et al.,* 2019). There did not appear to be any difference in the presence of these cells between the two hemispheres in any of the samples. Brightness and approximate interneuron density appeared to be constant across the optic tectum and between hemispheres. Overall, this is an indication that the OPN4L antibody was labelling all or most neurons in the sections.

While the potential for pan-neuronal expression is possible, it could also be an indication that there was an issue with the protocol causing non-specific binding. Despite the use of a blocking buffer in the immunolabelling protocol, blocking buffers typically work best if they are for the animal the secondary antibody was generated in. In this case that was the GFAP secondary antibody Alexa 488 as the blocking buffer used was goat serum and this secondary antibody was generated in a goat. The secondary antibody Alexa 555 which was used with the OPN4L and pas350 primary antibodies was generated in a donkey. While goat serum has also been reported to reduce background labelling due to reducing ionic and hydrophobic interactions, it may not have worked as well for the Alexa 555 secondary antibody. There is however an argument that blocking buffers do not need to be used at all, as some studies have identified no difference in background labelling levels when comparing using a goat serum blocking buffer step to a control with no blocking step included (Buchwalow *et al.,* 2011). The first antibody labelling was done using the 1:500 dilution of OPN4L as was determined from the retinal practice section, however this produced very strong signals that were present in the green channel as well. For this reason subsequent sections were done using a lower concentration of 1:1000 to ensure that actual labeling was being picked up and the signal was not due to issues such as primary antibody remaining on the sample or high levels of primary antibody leading to non-specific binding, both of which can cause strong signals and lead to signals showing up in the green channel (Buchwalow *et al.,* 2011). The decision to go from 20 μm sections to 40 μm was mainly done for ease of sectioning, but this would have had the same effect as weakening the dilution since the antibodies then had more tissue to spread through. Despite this, this concentration still may have been too high which could cause non-specific neuronal labelling. While pan-neuronal melanopsin expression is unlikely, the OPN4L antibody is producing clear labelling in these neurons.

Blood vessel labelling

Labelling of blood vessels was clear in the starry flounder sample labelled with pas350 but was not visible in the starry flounder samples labelled with the OPN4L antibody. DAPI staining allowed for clear blood vessel identification, as fish red blood cells contain nuclei which meant lines of oval shaped nuclei present in the samples were most likely blood vessels (Ribeiro *et al.,* 2023). Absence of red labelling in these regions of the OPN4L labelled samples indicates that the labelling seen in the pas350 sample may have been picking up on either *opn4m1* or *opn4m3,* although there is also the potential for non-specific blood vessel labelling which has been noted to be due to vascular components such as collagen and red blood cells (Buchwalow *et al.*, 2011). The periventricular grey area of the pas350 labelled starry flounder sample had clear labelling, although it appeared closer to the pas350 labelling seen in sablefish, both in this experiment and past work (Mokariasl, 2024). The periventricular grey labelling in the sablefish was in fewer cells than seen in the OPN4L labelled starry flounder. Those present in the sablefish were near the bottom of the periventricular grey area and did not appear to co-label with GFAP. In comparison to these results, the starry flounder labelled with pas350 notably did not have the labelling present along the top of the optic tectum or a clear pattern of labelling specifically localised to the bottom layer of neurons of the periventricular grey area. There also appeared to be fewer cells labelled in the periventricular grey in the starry flounder sample, indicating they may have also been blood vessels. Blood vessels have been shown to express melanopsin, which has been linked to photorelaxation in mice. Melanopsins in blood vessels are responsible for inducing vasodilation in response to UV or blue light stimuli (Sikka *et al.* 2014). Despite this, the much more likely explanation in this instance is non-specific immunolabelling. The absence of blood vessel labelling in the OPN4L labelled samples could then be explained by that antibody not having a sequence feature that may have caused the non-specific binding from the pas350 antibody (Buchwalow *et al.,* 2011).

Melanopsin expression in brains

Melanopsin expression has been characterised in the brains of several teleost fish including zebrafish, sablefish, the Japanese flounder, and salmon (Bellingham *et al.* 2002; Mokariasl, 2024; Liu *et al.,* 2020; Sandbakken *et al.,* 2012; Nakane *et al.,* 2013). The closest species to Starry flounder that has had melanopsin expression in the brain categorised through investigation into mRNA levels has been the Japanese flounder (*Paralichthys olivaceous*). Liu *et al.* (2020) included a number of non-visual opsins and tissues in their analysis however the primary goal of the study was identification and localisation of non-visual opsins in the retina of this species, so despite their results indicating a moderate level of *opn4m2* expression in brain tissue it was not mentioned in their discussion or investigated further in that work. Additionally, their work was aimed at overall mRNA expression levels and did not localise the expression to any specific neural structure or hemisphere. Some of the brighter patches near the hypothalamus in the OPN4L labelled starry flounder samples may have been melanopsin labelling. Sandbakken *et al.* (2012) identified melanopsin expression using in-situ hybridization in both the dorsal thalamus and in the nucleus lateralis tuberis of the hypothalamus in the Atlantic salmon (*Salmo salar*). Salmon could however have different expression patterns of opsins due to a recent whole genome duplication event in their lineage 80 million years ago. The authors also note asymmetrical expression of the *Xenopus*-like melanopsin in the habenula region. Nakane *et al.* (2013) identified melanopsin labelling in a bottom region of the masu salmon (*Oncorhynchus masou*) brain called the saccus vasculosus. This region appears as a dark red stripe on the dissected brains between the hypothalamus inferior lobes and was observed to be present in the starry flounder samples prior to embedding. While difficult to confirm, this region has many nuclei appearing in a characteristic pattern that appeared present in the section presented in Figure 7. This was identified in the starry flounder brain based on patterning in the DAPI staining found in the region. While there was only very faint OPN4L labelling noticed across this region in the sample, this may have been neuronal cell bodies. More relevant to our research, Nakane *et al.* (2013) also had faint labelling in the periventricular grey area using their melanopsin probe. The overall gene expression patterns of several opsin types that Nakane *et al.* (2013) looked for indicate that the saccus vasculosus is a structure associated with photoperiodism, which would explain the presence of opsins in the structure. The authors do not discuss melanopsin labelling in much detail or specify which paralogs their antibody bound, but their labelling appeared similar to that found in this study, indicating pan-neuronal labelling may be present for melanopsin in this species.

While all starry flounder caught in this experiment had undergone their complete metamorphosis, the age of the fish used in this study was unable to be determined. Due to their occupation of shallow water along with the transition from a pelagic to benthic lifestyle there are significant changes in the light levels experienced by an individual starry flounder throughout development, potentially exacerbated by the fact that during their development they also go from transparent to pigmented. There are several noted examples of the impacts of changing light stimulus on opsin expression. A study looking at quantification of melanopsin in immature vs mature male Japanese eels (Teleostei) found differential overall expression depending on age, considered to be due to the different depths occupied by individuals of the different life stages (Byun *et al.,* 2020). Additionally, visual opsins in the Japanese flounder (*P. olivaceous*) differ between life stages as the individuals transitions from pelagic to benthic (Zhang *et al.,* 2022). While there weren't starry flounder at different metamorphic stages used in this experiment, the time since this transition in each individual along with the specific extent of changes in opsin expression during and after development were unknown and may have confounded results.

Limitations

One limitation of the study was our inability to label with both melanopsin antibodies at once, as they both used the same secondary antibody. This prevented investigation into whether the regions that are being labelled by the OPN4L probe are also being picked up by the pas350 antibody as they should, since the pas350 antibody also binds *opn4m2*. One way that labelling using both primaries could be achieved would be using a different OPN4L antibody generated in another species, along with a different secondary antibody raised against the new species. It would also require a different excitation wavelength of the fluorophore conjugated to the secondary antibody than Alexa-555. Another limitation is the inability to quantify the levels of melanopsin expression in the optic tectum. While programs exist that could quantify the levels of fluorescence in the images obtained in this study, the focus was on getting images that clearly conveyed the presence or absence of expression. Along with changing section thickness and concentration, some imaging settings were not kept fully consistent between different samples (Table B2) preventing detection of smaller differences in brightness.

Future research

A key direction for future studies would be development of a protocol for quantifying levels of expression between the two hemispheres of the optic tectum. Quantification techniques such as qPCR techniques require knowledge of the mRNA or DNA sequence to use. Future sequencing work could be done to identify the *opn4m2* sequence in this species which would allow some of these techniques to be used. Mining the genome as was done by Liu *et al.* (2020) for *P. olivaceous* can be done for this species as sequence data is available. A qPCR technique would be better able to identify the presence of any small changes in expression between the two hemispheres that could not be discerned with a qualitative assessment. A more immediate direction for future research would be to do a series of concentration tests specifically with starry flounder brain tissue. This would allow for investigation into whether the concentration of the antibodies was too high and if that caused non-specific antibody labelling. Another would be repetition of the pas350 labelling on starry flounder to ensure that blood vessel labelling is indeed the only labelling present in the samples. Using qPCR for quantification along with immunohistochemical staining would paint the clearest picture of protein levels and their expression patterns in this species.

Conclusion

This study provided an investigation into melanopsin expression in the starry flounder and its potential regions of expression throughout the brain. Its presence as pan-neuronal labelling in the optic tectum indicates the potential for light sensitivity in this region of the brain. It also resulted in general observations of neuroanatomy and identification of radial glia and nuclei in the starry flounder, which had not previously been achieved. These data can serve as a baseline for future research in melanopsin expression in this species, as this species is a particularly useful model of light sensitivity due to its brain orientation and left and right sided polymorphism.

References

Bailes, H. J., and R. J. Lucas. 2009. Melanopsin and inner retinal photoreception. *Cellular and Molecular Life Sciences* **67**:99-111.

Beaudry, F. E. G., T. W. Iwanicki, B. R. Z. Mariluz, S. Darnet, H. Brinkmann, P.Schneider, and J. S. Taylor. 2017. The non-visual opsins: Eighteen in the ancestor of vertebrates, astonishing increase in ray-finned fish, and loss in amniotes. *Journal of Experimental Zoology Part B: Molecular and Developmental Evolution* **328**:685-696.

Bellingham, J., D. Whitmore, A. R. Philp, D. J. Wells, and R. G. Foster. 2002. Zebrafish melanopsin: Isolation, tissue localisation and phylogenetic position. *Molecular Brain Research* **107**:128-136.

Bergstrom, C. A. 2007. Morphological evidence of correlational selection and ecological segregation between dextral and sinistral forms in a polymorphic flatfish, *Platichthys stellatus*. *Journal of Evolutionary Biology* **20**:1104-1114.

Briñón, J. G., M. Médina, R. Arévalo, J. R. Alonso, J. M. Lara, and J. Aijón. 1993. Volumetric analysis of the telencephalon and tectum during metamorphosis in a flatfish, the turbot *Scophthalmus maximus. Brain, Behaviour and Evolution* **41**:1-5.

Buchwalow, I., V. Samoilova, W. Boecker, and M. Tiemann. 2011. Non-specific binding of antibodies in immunohistochemistry: fallacies and facts. *Scientific Reports* **1**. doi: 10.1038/srep00028

Byun, J.-H., J.-Y. Hyeon, E.-S. Kim, B.-H. Kim, H. Miyanishi, H. Kagawa, Y. Takeuchi, S.-J. Kim, A. Takemura, and S.-P. Hur. 2020. Gene expression patterns of novel visual and non-visual opsin families in immature and mature Japanese eel males. *PeerJ* **8**. doi:10.7717/peerj.8326

Davies, W. I. L., L. Zheng, S. Hughes, T. K. Tamai, M. Turton, S. Halford, R. G. Foster, D. Whitmore, and M. W. Hankins. 2011. Functional diversity of melanopsins and their global expression in the teleost retina. *Cellular and Molecular Life Sciences* **68**:4115-4132.

Davies,W. I.L., T. K. Tamai, L. Zheng, J. K. Fu, J. Rihel, R. G. Foster, D. Whitmore, and M. W. Hankins. 2015. An extended family of novel vertebrate photopigments is widely expressed and displays a diversity of function. *Genome Research* **25**:1666-1679.

Geffen, A.J., H. W. van der Veer, and R. D. M. Nash. 2007. The cost of metamorphosis in flatfishes. *Journal of Sea Research* **58**:35-45.

Graf, W., and R. Baker. 1990. Neuronal adaptation accompanying metamorphosis in the flatfish. *Journal of Neurobiology* **21**:1136-1152.

Güler, A. D., J. L. Ecker, G. S. Lall, S. Haq, C. M. Altimus, H.-W. Liao, A. R. Barnard, H. Cahill, T. C. Badea, H. Zhao, M.W. Hankins, D. M. Berson, R. J. Lucas, K.-W. Yau and S. Hattar. 2008. Melanopsin cells are the principal conduits for rod–cone input to non-image-forming vision. *Nature* **453**:102–105.

Isa, T., E. Marquez-Legorreta, S. Grillner, and E. K. Scott. 2021. The tectum/superior colliculus as the vertebrate solution for spatial sensory integration and action. *Current Biology* **31**:R741-R762.

Kang, D.-Y., J.-H. Lee, W.-J. Kim, and H.-C. Kim. 2012. Morphological specificity in cultured starry flounder *Platichthys stellatus* reared in artificial facility. *Fisheries and Aquatic Sciences* **15**:117-123.

Kang, D.-Y., S.-G. Byun, J.-I. Myeong, H.-C. Kim, and B.-H. Min. 2014. Morphological analysis of blind-side hypermelanosis of the starry flounder, *Platichthys stellatus* during early development. *Development and Reproduction* **18**:79–87.

Kyle, H. M. 1923. The asymmetry, metamorphosis and origin of flat-fishes. *Philosophical Transactions of the Royal Society B Biological sciences* **211**: 75–129.

Lindsey, B.W., G.E. Aitken, J.K. Tang. M. Khabooshan, A. M. Douek, C. Vandestadt and J. Kaslin. 2019. Midbrain tectal stem cells display diverse regenerative capacities in zebrafish. *Scientific Reports* **9**. doi:10.1038/s41598-019-40734-z

Liu, Y. W. Zhang, X. Du, Y. Liu, J. Qu, X. Liu, J. Liu, and Q. Zhang. 2020. Genome-wide identification of nonvisual opsin family reveals amplification of RPE-retinal G protein receptor gene (RGR) and offers novel insights into functions of RGR(s) in *Paralichthys olivaceus*

(*Paralichthyidae*, Teleostei). *Journal of Experimental Zoology Part B: Molecular and Developmental Evolution* **334**. doi: 10.1002/jez.b.22914

Lü, Z., L. Gong, Y. Ren, Y. Chen, Z. Wang, L. Liu, H. Li, X. Chen, Z. Li, H. Luo, H. Jiang, Y. Zeng, Y. Wang, K. Wang, C. Zhang, H. Jiang, W. Wan, Y. Qin, J. Zhang, L. Zhu, W. Shi, S. He, B. Mao, W. Wang, X. Kong, and Y. Li. 2021. Large-scale sequencing of flatfish genomes provides insights into the polyphyletic origin of their specialized body plan. *Nature Genetics* **53**:742-751.

Mokariasl, N. 2024. Quantification of melanopsin gene expression during sablefish (*Anoplopoma fimbria*) development and spatial mapping of *opn4m* proteins on a newly established brain atlas. University of Victoria, Victoria, BC.

Munroe T. A. 2005. Systematic diversity of the Pleuronectiformes. Pp. 10–41 in: Flatfishes: biology and exploitation, Gibson RN, editor. Blackwell, Oxford.

Nakane, Y., K. Ikegami, M. Iigo, H. Ono, K. Takeda, D. Takahashi, M. Uesaka, M. Kimijima, R. Hashimoto, N. Arai, T. Suga, K. Kosuge, T. Abe, R.Maeda, T. Senga, N. Amiya, T. Azuma, M. Amano, H. Abe, N.Yamamoto, and T. Yoshimura. 2013. The saccus vasculosus of fish is a sensor of seasonal changes in day length. *Nature Communications* **4**. doi: 10.1038/ncomms3108.

Provencio, I., G. Jiang, W. J. De Grip, W. Pär Hayes, and M. D. Rollag. 1998. Melanopsin: An opsin in melanophores, brain, and eye. *Proceedings of the National Academy of Sciences of the United States of America* **95**:340-345.

Ribeiro, A., M. Rebocho da Costa, C. de Sena-Tomás, E. Charas Rodrigues, R. Quitéria, T. Maçarico, S. Constantino Rosa Santos, and L. Saúde. 2023. Development and repair of blood vessels in the zebrafish spinal cord. *Open Biology* **13**. doi:10.1098/rsob.230103

Sandbakken, M., L. Ebbesson, S. Stefansson, and J. V. Helvik. 2012. Isolation and characterization of melanopsin photoreceptors of Atlantic salmon (Salmo salar). *Journal of Comparative Neurology* **520**:3727-3744.

Sikka, G., G. P. Hussmann, D. Pandey, S. Cao, D. Hori, J. T. Park, J. Steppan, J. H. Kim, V. Barodka, A. C. Myers, L. Santhanam, D. Nyhan, M. K. Halushka, R. C. Koehler, S. H. Snyder, L. A. Shimoda, and D. E. Berkowitz. 2014. Melanopsin mediates light-dependent relaxation in blood vessels. *Proceedings of the National Academy of Sciences of the United States of America* **111**:17977–17982.

Sohn, M.-Y., G. Kang, K.-H. Kim, H.-J. Son, and C.-I. Park. 2025. Molecular adjuvant potential of GCSF and MCSF in starry flounder challenged with *Streptococcus parauberis. Animals* **15**. doi:10.3390/ani15131848

Zhang, Z., Y. Liu, W. Zhang, X. Du, and J. Liu. 2022. Benthic visual adaptation by fine-tuning light sensitivity in Japanese flounder (*Paralichthys olivaceus*). *Frontiers in Marine Science* **9**. doi:10.3389/fmars.2022.1019660

Zheng, W., C. Liu, S. Han, T. Wang, T. Yang, Z. Liu, D. Xu, H. Han, X. Xi, C. Shao and K. Liu. 2025. Chromosome-level genome assembly of starry flounder (*Platichthys stellatus*) *Scientific Data* **12**. doi:10.1038/s41597-025-05525-4

Appendix A: Antibody labelling protocol

Primary antibody labelling

Slides were removed from storage at -70ºC and thawed for five minutes. Slides were then washed in 1X PBS for 10 minutes. Slides were then dried with a kimwipe and a small circle was drawn around slides with a PAP pen (Liquid Blocker Super PAP Pen Mini, Daido Sangyo Co., Ltd. Japan, Newcomer Supply Cat. No. 6506). 1% triton in 1X PBS was added to samples and left to incubate for 15 minutes. 1% triton in 1X PBS was removed by pipette and samples were washed with 1X PBS 2 times via pipette. Slides were then submerged in 1X PBS for 5 minutes. A blocking buffer (1X PBS with 2% goat serum) was added to the samples and left to incubate for 30 minutes. Primary antibody dilutions were prepared using 1X PBS and added to samples. Samples were left overnight to incubate at 4ºC.

Secondary antibody labelling

Slides were washed twice with 1X PBS using a pipette. Slides were then submerged in 1X PBS for 5 minutes. Slides were submerged in fresh 1X PBS and left for an additional 5 minutes. This was repeated for a total of 3 washes. Secondary antibody dilutions were prepared with 1X PBS and added to samples. Samples were left to incubate at room temperature for 2 hours. Slides were washed twice with 1X PBS using a pipette. Slides were then submerged in 1X PBS for 5 minutes. Slides were submerged in fresh 1X PBS and left for an additional 5 minutes. This was repeated for a total of 3 washes. Slides were mounted using DAPI and coverslips were added. Slides were sealed with nail polish and stored at 4ºC.

Appendix B: Sample measurements and imaging settings

Table B1. Starry flounder size measurements from tip of snout to tail

Sample figure number	Size (cm)
7 and 12	8.7
Not sectioned/labelled	12.6
11	13.5
Not sectioned/labelled	20.9
13	21.2
9	11.1
10	11.1
Not labelled	12.4
11	13.8

Table B2. Imaging settings for Nikon C2 confocal microscope.

Sample figure number	561 nm laser power/HV (red)	488 nm laser power/HV (green)	405 nm laser power/HV (blue)	Z-stack range (µm)	steps
4	0.64/72	0.64/70	2.07/77	3.5	3
5	0.85/69	0.85/71	1.74/79	9.73	4
6	1.25/78	1.08/74	1.08/79	5.14	3
7 and 12	1.00/75	1.85/79	1.85/77	4.23	3
8	0.85/69	1.00/60	1.35/74	10.62	8
9	1.74/74	1.54/75	1.08/79	13.4	4
10	1.35/68	1.44/67	1.35/79	5.4	3
11	1.00/73	0.71/73	1.96/75	3.05	2
13	1.74/76	1.54/75	1.08/79	6.23	3